Biochemical and Biophysical Research Communications 445 (2014) 71–77

Contents lists available at ScienceDirect

Biochemical and Biophysical Research Communications

journal homepage: www.elsevier.com/locate/ybbrc

Down regulated connexin26 at different postnatal stage displayed different types of cellular degeneration and formation of organ of Corti

Sen Chen [a], Yu Sun [a,*], Xi Lin [c], Weijia Kong [a,b,*]

[a] Department of Otolaryngology, Union Hospital, Tongji Medical College, Huazhong University of Science and Technology, Wuhan 430022, PR China
[b] Institute of Otorhinolaryngology, Tongji Medical College, Huazhong University of Science and Technology, Wuhan 430022, PR China
[c] Department of Otolaryngology, Emory University School of Medicine, 615 Michael Street, Atlanta, GA 30322-3030, USA

ARTICLE INFO

Article history:
Received 23 January 2014
Available online 31 January 2014

Keywords:
Connexin26
Cell degeneration
Hair cells
Mouse models
Genetic deafness

ABSTRACT

Connexin26 (Cx26) mutation is the most common cause for non-syndromic hereditary deafness. Different congenital Cx26 null mouse models revealed a profound hearing loss pattern and developmental defect in the cochlea. Our study aimed at establishing a Cx26 knocking down mouse model at different postnatal time points and to investigate the time course and pattern of the hearing loss and cell degeneration in these models. Morphologic changes were observed for 5 months to detect long-term diversities among these models. Depending on the time point when Cx26 expression was reduced, mild to profound hearing loss patterns were found in different groups. Malformed organ of Corti with distinct cell loss in middle turn was observed only in early Cx26 reduction group while mice in late Cx26 reduction group developed normal organ of Corti and only suffered a few hair loss in the basal turn. These results indicated that Cx26 may play essential roles in the postnatal maturation of the cochlea, and its role in normal hearing at more mature stage may be replaceable.

1. Introduction

Connexin26(Cx26) mutations account for up to 50% of the human non -syndromic hereditary deafness cases, which is considered as one of the most common human birth defects [1–3]. To date, more than 90 mutations have been identified in the Cx26 gene [4]. Most of Cx26 mutations cause severe hearing loss inherited recessively.

To explore the deafness mechanism in Cx26 mutants, different transgenic mouse models had been established for investigation. By crossbreeding of $Cx26^{loxP/loxP}$ and Otog-Cre mice, the embryonic lethality of Cx26 knockout (KO) mice was overcome by restricting the Cx26 deletion region specifically in the inner ear in 2002 [5]. The inner ear of this $Cx26^{loxP/loxP}$; Otog-Cre mice developed normally, but by the postnatal day 14 (P14), cell death was firstly observed in the supporting cell (SC) adjacent to the inner hair cell (IHC) and extended later to outer hair cell (OHC). Another line of transgenic mice with a dominant-negative Cx26 were generated in 2003, and the mice showed severe to profound hearing loss, failure in the formation of the tunnel of Corti (TC) and degeneration of sensory hair cells [6]. Moreover, by use of Cre-loxP system, more and more spatially-specific Cx26 KO mice were generated. The KO patterns in these mice depend on the expression time and location of the promoter gene. The $Cx26^{loxP/loxP}$; foxg1-Cre and $Cx26^{loxP/loxP}$; pax2-Cre mice were two spatially-specific Cx26 KO mice with Cx26 deletion at embryonic day 8.5 in otic placode [7]. These mice showed severe hearing loss, failure in the opening of the TC, OHC loss at P13 and then massive cell death in both middle and basal turns [8]. Compared to these spatially-specific Cx26 KO mice, another kind of conditional Cx26 (cCX26) null mice showed similar pathological change by tamoxifen injection at embryonic day 19 (E19) [9]. The reduction in Cx26 expression started at the time of tamoxifen injection, thus this line of mouse model is considered as the time-specific Cx26 knocking down model. Although the exact deafness mechanism remains speculative, substantial evidence from different models support that Cx26 deficiency can arrest the cochlea development before the cell degeneration, which indicated that Cx26 plays a developmental function during the postnatal maturation of the sensory epithelium of the cochlea [8]. The postnatal maturation is a series of cell differentiation

Abbreviations: Cx26, connexin26; KO, knockout; KD, knockdown, SC, supporting cell; IHC, inner hair cell; OHC, outer hair cell; TC, tunnel of Corti; TMX, tamoxifen; ABR, auditory brainstem response.

* Corresponding authors. Fax: +86 27 85776343 (Y. Sun). Address: Department of Otolaryngology, Union Hospital, Tongji Medical College, Huazhong University of Science and Technology. Fax: +86 27 85776343 (W. Kong).

E-mail addresses: sunyu@hust.edu.cn (Y. Sun), entwjkong@hust.edu.cn (W. Kong).

http://dx.doi.org/10.1016/j.bbrc.2014.01.154
0006-291X/

associated with the Cx26 increase [10,11]. However, the previous Cx26 KO patterns are limited to the specific promoter as pax2 or foxg1 that triggers Cx26 reduction in embryonic time. More flexible Cx26 deletion patterns are needed to investigate the Cx26 functions in developmental process. Thus, the timed cC26 null mice become the best candidate for the Cx26 postnatal knocking down model.

In this study, we knocked down the Cx26 at a series of postnatal time points by using cCx26 null mice. A five-month observation was performed to determine the diverse time courses of hearing loss and cell degeneration patterns among these groups. Our data suggests that accurate timing of early postnatal Cx26 expression is the fundamental prerequisite for cochlear maturation and normal hearing.

2. Materials and methods

2.1. Mouse models

$Cx26^{loxP/loxP}$ mice and $Rosa26^{CreER}$ mice were provided by Prof. Lin Xi at the Emory University. Mice were raised in specific-pathogen free experiment animal center of Huazhong University of Science and Technology. Crossbreeding of the above mice generated $Cx26^{loxP/loxP}$; $Rosa26^{CreER}$ mice. Details of these transgenic mice could be found in Prof. Lin's publication [9]. Briefly, the entire coding sequence of Cx26 was expected to be removed by the activation of Cre recombinase which was induced in the presence of synthetic estrogen antagonist tamoxifen (TMX). In our studies, the time-specific conditional Cx26 null mouse model was generated by a single subcutaneous injection of TMX diluted in fat emulsion (1.5 mg/10 g body weight, T5648-1G, Sigma–Aldrich, St. Louis, MO) to $Cx26^{loxP/loxP}$; $Rosa26^{CreER}$ mice in the postnatal day 1, 6 and 12 (P1, P6 and P12). In our preliminary experiment, $Cx26^{loxP/loxP}$; $Rosa26^{CreER}$ mice received fat emulsion injection at different time points, and all mice displayed unaffected normal hearing. We therefore used mice with P1 fat emulsion injection as control. All experimental procedures were conducted in accordance with the policies of the Committee on Animal Research of Tongji Medical College, Huazhong University of Science and Technology.

2.2. Assessment of hearing function

Auditory brainstem response (ABR) was measured at the 1, 3 and 5 month after birth. Mice ($n = 8–10$ for each group) were anaesthetised with ketamine (120 mg/kg, i.p.) and chloropromazine (20 mg/kg, i.p.), and then a heating pad was used to keep them warm in a sound-attenuating chamber. A sound delivery tube connected to a loudspeaker (Tucker-Davis Technologies, Alachua, FL, USA) was fitted to external auditory canal of mouse ear. Tone burst stimuli were generated by Tucker-Davis Technologies (TDT) System at frequencies of 8 kHz, 16 kHz, 24 kHz and 32 Hz, then the responses were amplified and averaged for 1024 times. The lowest sound level that elicited a repeatable wave was considered as the threshold.

2.3. DNA and RNA preparation and quantitative RT- PCR

Mouse tails from the pups were used to detect the genotype of the crossbreeding mice. Details could be found in Sun's publication [9]. The mRNA expression level of Cx26 was checked by quantitative real-time PCR. Membranous labyrinth of cochleae from 1 month old mice ($n = 6$ for each group) of experimental and control groups were dissected carefully on ice. RNA were extracted with Total RNA Kit I (Omega, USA) by standard procedures. The cDNA was reverse transcribed using a PrimeScript RT reagent Kit with gDNA eraser (TaKaRa, Japan). Primer pairs for Cx26 and β-actin were as follows: Cx26 forward 5′-ACAGAAATGTGTTGGT GATGG-3′; reverse 5′-CTTTCCAATGCTGGTGGAGTG-3′ and β-actin forward 5′-CATCCGTAAAGA CCTCTATGCCAAC-3′; reverse 5′-ATGGACCACCGATCCACA-3′. Real-time PCR was performed by use of SYBER Green PCR Technology in Roche LightCycler® 480 instrument on the following conditions: 95 °C for 5 min, 40 cycles of 95 °C for 20 s, 56 °C for 20 s, 72 °C for 40 s. A melting curve analysis performed by LightCycler® 480 system was used to evaluate the specificity and the integrity of the PCR products. The relative mRNA expression of experimental and control groups were calculated by using $2^{-\Delta\Delta Ct}$ method.

2.4. Western blot analysis

The Cx26 protein level was determined by Western blot analysis. Membranous labyrinth of the cochleae from both experimental and control groups ($n = 5$ for each group) were carefully dissected on ice. The total protein was extracted using RIPA lysis buffer (Beyotime, Haimen, China) by following the manufacturer's instructions. For this analysis, proteins (10 μg per lane) were separated by electrophoresis on a 12% sodium dodecyl sulphate (SDS) polyacrylamide gel and then transferred to polyvinylidene difluoride (PVDF) membranes. Bands were incubated in a blocking solution (TBST containing 5% milk) for 1 h. Proteins of Cx26 and β-actin were detected by using polyclonal antibodies against Cx26 (Cat. No. 710500, 1:500, Invitrogen, USA) and polyclonal antibodies against β-actin (Cat. No. 04-1116, 1:1000, Millipore, USA), respectively. After washing in TBST, bands were incubated for 1 h at room temperature with horseradish peroxidase (HRP)-conjugated secondary antibody. Protein bands were visualized using the ECL reaction kit (Beyotime, Haimen, China) according to the manufacturer's instructions by exposure on medical film. The Cx26 protein levels were measured by the Quantity One 4.6.2 Software (Bio-Rad, USA) and normalized to the level of β-actin in corresponding lanes.

2.5. Cochlear tissue preparation and morphological examination

Animals were deeply anesthetized with a combination of katamine and chlorpromazin by intraperitoneal injection and perfused transcardially with 4% paraformaldehyde in phosphate-buffered saline (PBS). The cochleae were carefully dissected from the temporal bones and kept in the same fixative at 4 °C overnight. After decalcification with disodium EDTA, the cochleae were dehydrated sequentially in graded alcohol, embedded in paraffin by conventional protocol. Sections with a thickness of 5 μm were cut for morphological examination.

Three animals from each group were used for SGN counting. Two neighboring sections with hematoxylin-eosin (HE) staining separated by 40 μm were used to avoid double counting. The area of the Rosenthal's canal was measured with Image Pro Plus 6.0 software from the cochlear sections, and the neurons with distinct nucleus were taken into counting. Counting errors were corrected by using the Abercrombie's formula: $T/T + D$, in which T is the section thickness and D is the mean diameter of the SGN [12].

For flattened cochlear preparation, the cochleae ($n = 3$ for each group) after decalcification were carefully dissected out under a stereomicroscope and three portions of the basilar membrane from the apical, middle and the basal turn were used for hair cell staining. The samples, permeabilized with 0.3% Triton X-100 in 0.01 M PBS for 5 min, were stained with 4′,6-diamidino-2-phenylind-ole (DAPI) for 5 min. The images of each cochlea turn were obtained with a laser scanning confocal microscope sequentially (Nikon, Japan). To get the cochleogram, the hair cells were counted in 12 consecutive fields from the apex to the basal part of the samples. The last basal part of the basilar membrane was hard to obtain.

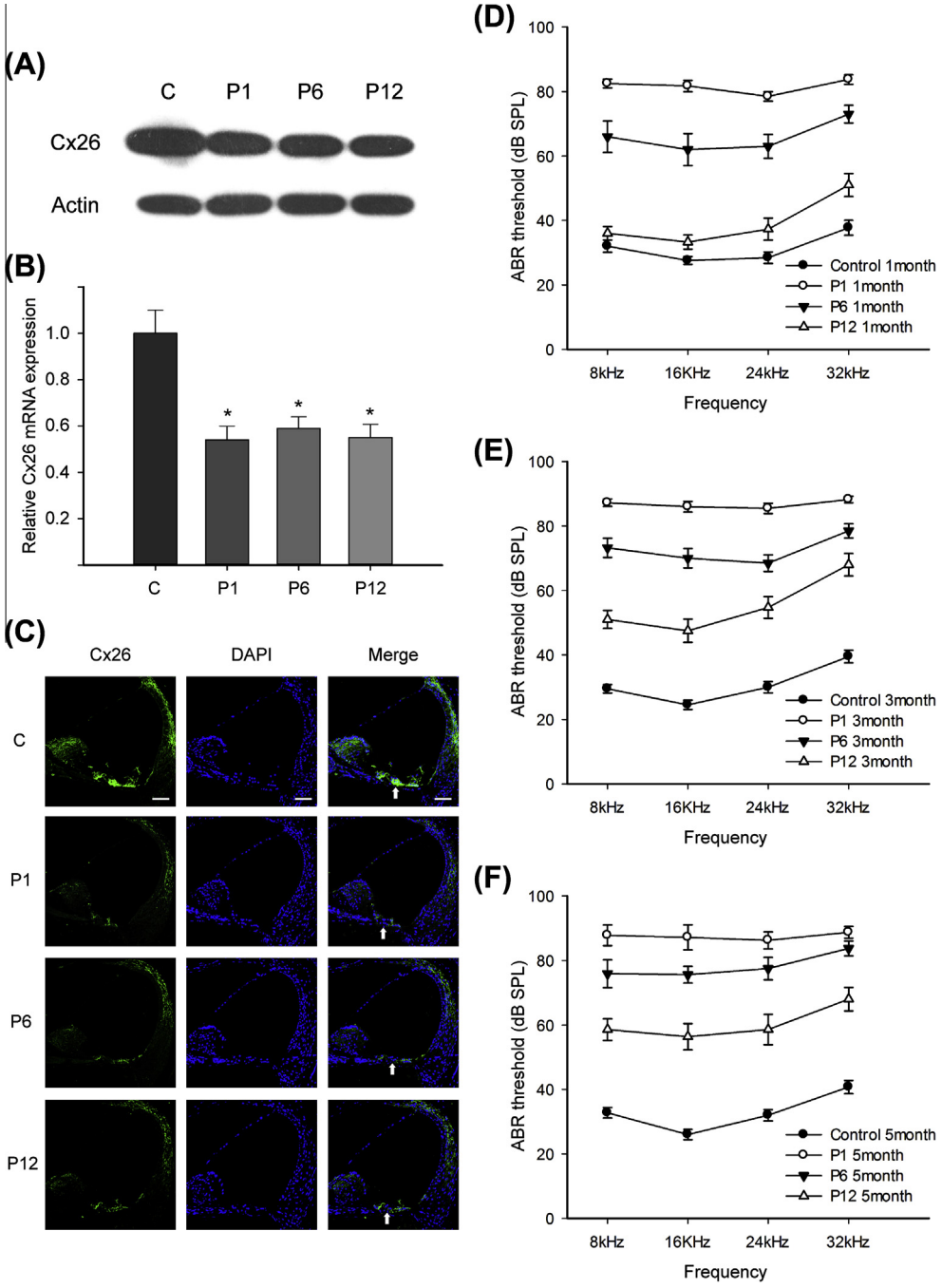

Fig. 1. Summary of data validating different Cx26 KD mice models and hearing loss patterns in this study. (A) Western blots measuring Cx26 in the cochleae of 1 month old mice from control and different experimental groups. (B) RT-PCR measuring Cx26 mRNA in the cochleae of 1 month old mice from control and different experimental groups. (C) Immunolabeling of Cx26 in the cochleae of 1 month old mice from control and different experimental groups. Scales represent approximately 40 μm. (D–F) Auditory thresholds were measured at the one (D), three (E) and 5 months (F) after birth, respectively. Legends for different groups are given in the panel. $^{*}P < 0.05$ when compared to the control group.

The counted portion contained about 90 percents of the whole basilar membrane of the mouse cochlea.

2.6. Immunofluorescent labeling

After deparaffinization, rehydration, antigen retrieval and non-specific antigen site blocking by conventional protocol, samples were incubated with polyclonal antibodies against Cx26 (Cat. No. 710500, dilution factor 1:100, Invitrogen, USA) at 4 °C overnight. Cx26 protein and the nucleus were stained by a fluorescently tagged secondary antibody for an hour and DAPI for 5 min at room temperature, respectively. Images were taken with a laser scanning confocal microscope (Nikon, Japan).

2.7. Statistics analysis

Data were expressed as mean ± SEM and plotted by SigmaPlot software. Statistical analysis was performed by One-way analysis of variance (ANOVA) with SPSS 17.0 software. The least significant difference (LSD) post hoc test was used to compare differences

between two of the groups. In all analysis, a $^{*}P < 0.05$ was considered statistically significant.

3. Results

3.1. Decreased Cx26 in mRNA and protein level induced by Cx26 deletion

Compared to control the group, the Cx26 mRNA were significantly decreased in all experiment groups (Fig. 1B). The relative Cx26 mRNA expression in P1, P6 and P12 KD groups were 54.2 ± 6.8%, 59.5 ± 5.0% and 55.3 ± 5.8%, respectively. There was no statistically significant differences among the experimental groups. The Cx26 protein level in 1 month old mice showed similar changes (Fig. 1A). In comparison with the control group, the Cx26 protein level in P1, P6 and P12 KD groups were 58.6 ± 6.7%, 62.0 ± 7.2% and 62.8 ± 6.0%, respectively. There was statistically significant differences between experimental and control groups but not among experimental groups. As shown in Fig. 1C, the Cx26 staining (green) was detected in the organ of Corti, lateral wall and spiral limbus in the control group. In 1 month old mice of P1, P6 and P12 KD groups, there were a distinct Cx26 reduction in the organ of Corti (white arrow, Fig. 1C).

3.2. Different time courses of hearing loss pattern induced by Cx26 deletion at different postnatal time points

ABRs of all the mice were measured at the postnatal month 1, 3 and 5 (Fig. 1D–F). The control group showed a stable normal hearing in the observations. The ABR thresholds in the P1 KD group were high around 90 dB SPL at all the time points tested. In comparison to P1 KD group, the hearing loss of P6 KD group was over a whole-frequency range and gradually aggravated to around 80 dB SPL in the 5th month. Interestingly, the hearing loss in the P12 KD group displayed a mild deafness at first, but gradually worsened in the next few months.

3.3. Different cell degeneration patterns induced by Cx26 deletion at different postnatal time points

The paraffin sections with HE staining were used in morphologic studies (Fig. 2). The panel A (Fig. 2A) showed a full view of a cochlea, and the organ of Corti in middle turn (black frame, Fig. 2A) was amplified for further investigation. As shown in Fig. 2B, F and J, the organ of Corti (middle turn, the same below) in the control group obtained at different time points had no significant deformity and cellular degeneration. The tunnel of Corti (arrowhead, Fig. 2B) was open and the IHCs were intact (arrows, Fig. 2B). At the age of 1 month, the TC was closed in P1 KD group (arrowhead, Fig. 2C), while mice in P6 and P12 KD groups developed an architecturally normal organ of Corti (Fig. 2D and E). At the age of 3 month, the hair cell and supporting cell degeneration were clearly shown in P1 and P6 KD groups (Fig. 2G and H), while the HCs and SCs were intact in P12 KD group (Fig. 2I). Compared to the disintegration of organ of Corti in 5 month old mice of P1 and P6 KD groups (Fig. 2K and L), the peer in P12 KD group had no distinct deformity and cell degeneration (Fig. 2M).

3.4. Different HC and SGN loss patterns induced by Cx26 deletion at different postnatal time points

HC counting was investigated by whole-mount preparation (Fig. 3). Severe HC loss was observed in the middle turn of P1 and P6 KD groups at 1 month, and this situation worsened gradually (Fig. 3A, C and E). At the age of 3 month, the HC degeneration enlarged to basal turn in P1 and P6 KD groups. The out hair cell was more vulnerable than inner hair cell in all experimental groups. 1 month old mice in P12 KD group showed almost no HC loss, but a moderate OHC loss in basal turn was observed and aggravated from 3 month after birth. Details of the patterns and time courses of HC degeneration are given in Fig. 3B, D and F.

SGN degeneration was quantified by SGN counting. In 1 month old mice of P1 and P6 KD groups, a mild SGN loss was observed in the middle turn (Fig. 4A and B). Three month after birth, the SGN lesion enlarged to apical and basal turn in P1 and P6 KD groups (Fig. 4C and D). By 5 months, more than half of SGNs from the middle and basal turns in P1 KD group disappeared and P6 KD group also suffered a significant SGN loss in the corresponding turn (Fig. 4E and F). The clustering of SGNs were observed in the P1 or P6 KD group (arrow, Fig. 4E, Apical, P1 deletion group). To the contrary, P12 KD group had minimum SGN loss in all regions of the cochlea (Fig. 4). Details of the patterns and time courses of SGN degeneration are given in the Fig. 4B, D and F.

4. Discussion

In this study, we successfully knocked Cx26 down at a series of postnatal time points in the cCx26 null mice, and observed different time courses and patterns of hearing loss and cell degeneration in this mouse model. Compared to previous congenital KO or KD models, these postnatal KD models showed diversified phenotypes. In P1 KD group, the mice showed a profound hearing loss, failure in opening the TC in the middle turn and massive cell degeneration. The injury pattern of P1 KD group was similar to previous time-specific knocking down model with Cx26 deletion at E19 [9]. Among these changes, deformity of the TC was a common landmark in the Cx26 null mice. According to previous theory, specific loss of these structures in the organ of Corti was considered to

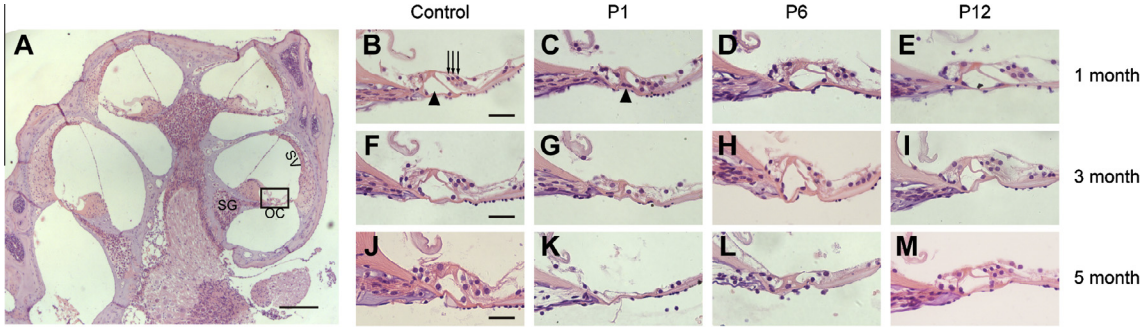

Fig. 2. Morphology of the organ of Corti at the middle turn in control and different experimental groups. (A) A full view of a cochlea obtained from the control group. Abbreviations: SV: stria vascularis; OC: organ of Corti; SG: spiral ganglia. Morphology of the OC in 1 month (B–E), three month (F–I) and 5 month (J–M) old mice from control and different experimental groups. Scales in panel A and panel B represent approximately 200 μm and 40 μm, respectively.

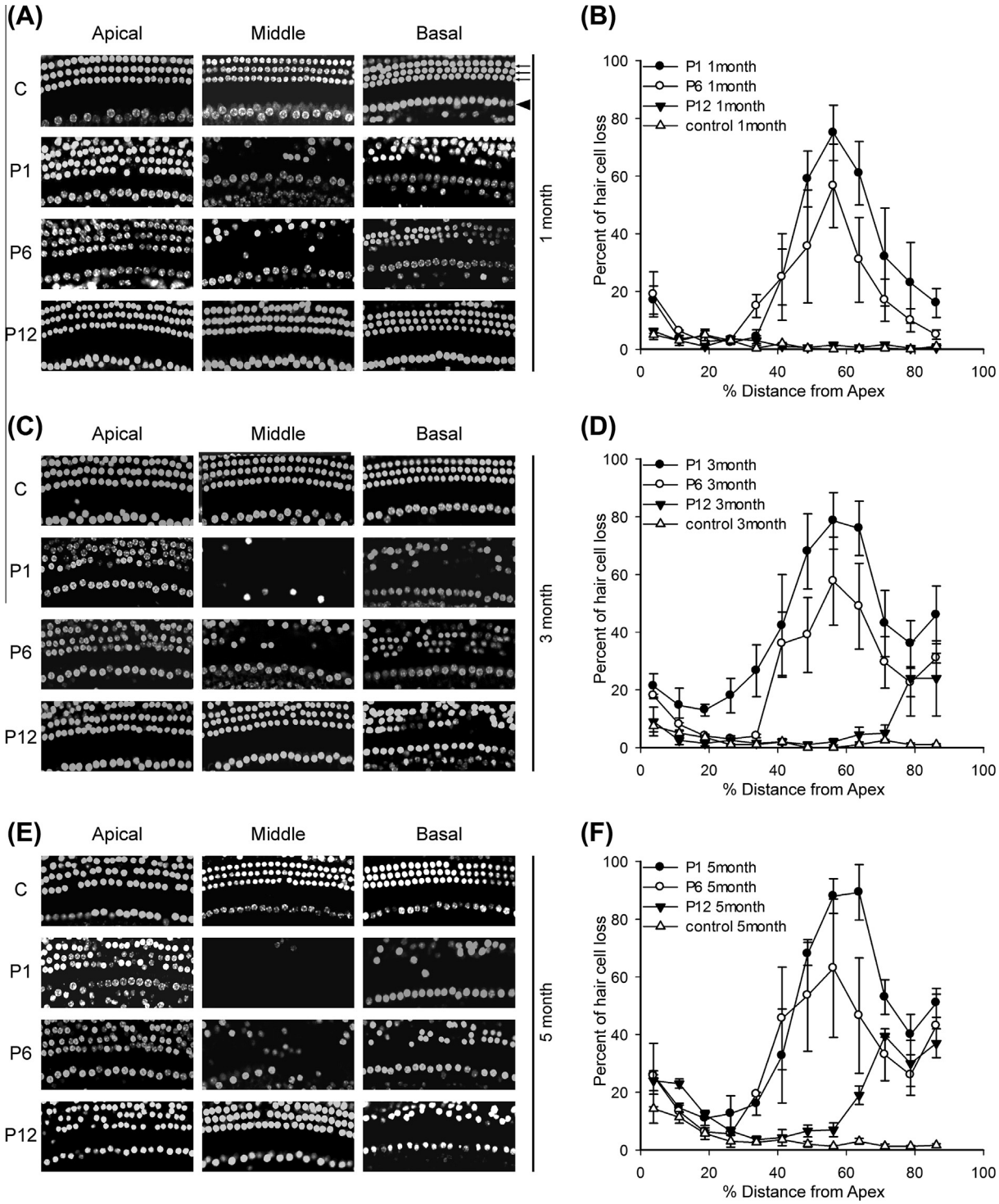

Fig. 3. Patterns and time courses of HC loss in different Cx26 KD groups. Panels (A, C and E) show examples of HC nuclei stained with DAPI from control and different experimental groups. Three rows of OHCs (arrow, Panel A) are on the top and one row of IHC (arrowhead, Panel A) are at the bottom. Panels (B, D and F) show the quantifications of HC loss at specific cochlear locations for different Cx26 KD groups. Legends for different groups are given in the panels.

cause profound hearing loss [13]. However, the TC of Cx26 null mice in P6 and P12 KD group developed normally, which indicates that certain amount of Cx26 expression in the postnatal P1 to P6 is a key factor for the formation of TC. Although the TC successfully opened in P6 KD group, the mice still suffered severe hearing loss and HC death accompanying with subsequent SGN loss. The evidence suggested that other late-onset deafness mechanisms that involved in P6 KD group still need to be investigated. Additionally, the HC and SGN loss in P1 and P6 KD groups aggravated from middle to basal turn in the following 5 months after birth. This gradually worsened degeneration pattern was also observed in cCx26 null mice with Cx26 deletion at E19 [9]. Wang et al. reported that the HC was born intact and HC loss was not noticed until P13 in the cCx26 null mice. All these observations indicated that deletion Cx26 at an early postnatal time may induce distinct cell loss in the cochlea. A current hypothesis is that gap junction undertakes

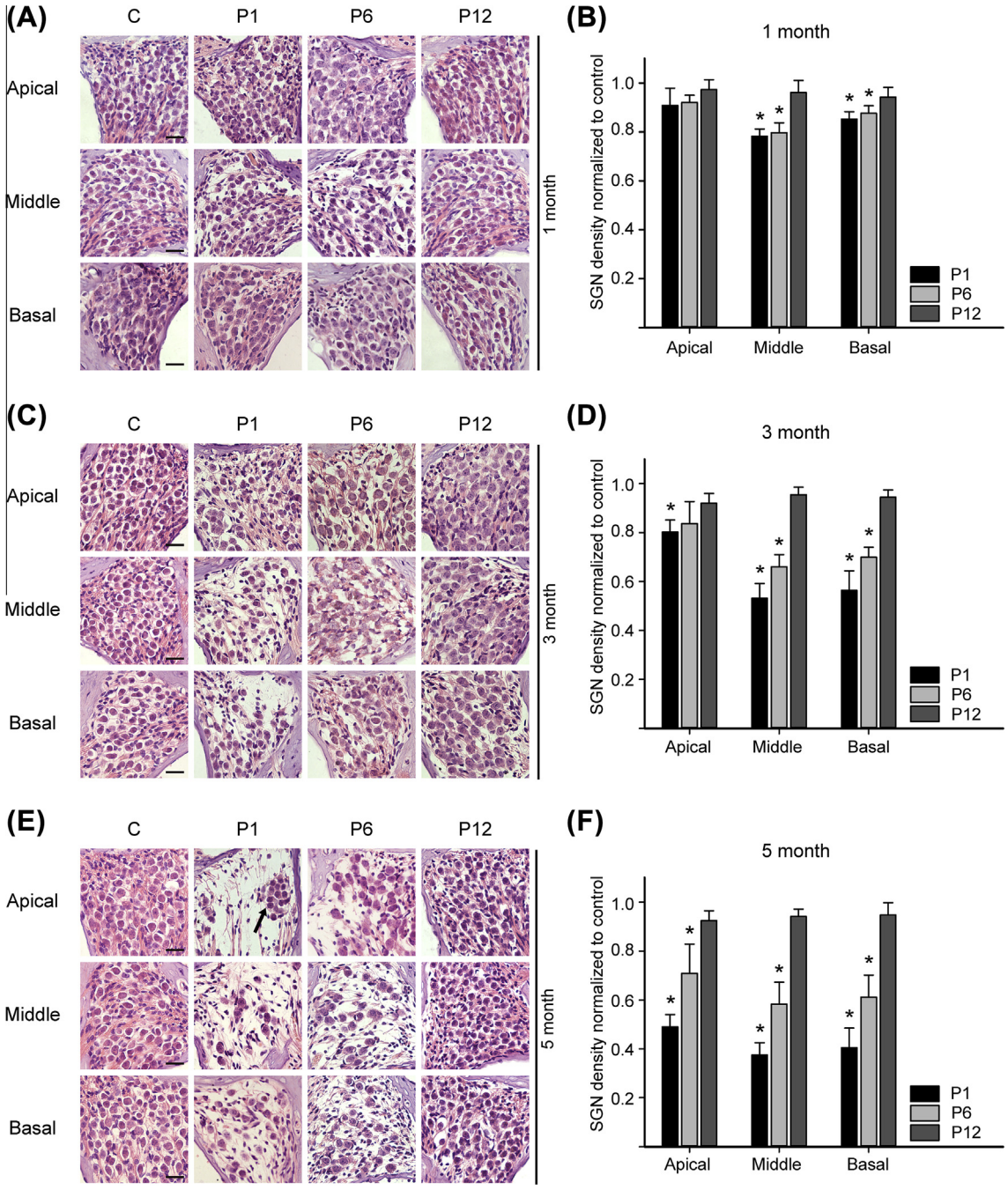

Fig. 4. Patterns and time courses of SNG loss in different Cx26 KD groups. Panels (A, C and E) show examples of SGN stained with hematoxylin-eosin from control and different experimental groups. Scales represent approximately 30 μm. Panels (B, D and F) show the relative survival of the SGN at specific cochlear locations for different Cx26 KD groups. Legends for different groups are given in the panels. $^{*}P < 0.05$ when compared to the control group.

the transportation of the glucose and vital molecules into the cochlea, however, other mechanisms of HC death in this model still need more investigation [14,15].

The mouse cochlea is born immature and can not respond to sound until P14 [10,16]. Chu Liang et al. have found that no ABR was detectable from P14 in Cx26 KO mice while severe HC loss and SGN degeneration appeared relative late [17]. In comparison to the severe deafness in P1 and P6 KD groups, that P12 KD group showed a mild hearing loss pattern is not surprising. Additionally, the cell loss in P12 deletion group was also less profound than that in P1 and P6 KD groups. A potential explanation is that the cochlea soon to be mature may be more resistant to the Cx26 deficiency. Considering all these factors, we speculated that only knocking down Cx26 at early postnatal time points had disrupted the normal development of cochlea which led to distinct deafness patterns.

More recently, Cx26 gene therapy has been applied to cochlear organotypic culture from Cx26 null mouse at P5. Giulia Crispino et al. transducted of these cultures with a bovine adeno associated virus vector, which had restored connexin26 protein expression and rescued gap junction coupling in these cultures [18]. Moreover, Wang et al. found that early postnatal virus incubation (before P5) to the scala media can preserve the auditory function in normal mice [19]. These findings also demonstrated invasive gene therapy should be achieved before the P5 for the sake of

hearing protection. Our data indicated the postnatal Cx26 expression at P1 to P6 is vital for the normal hearing formation. Yu et al. have successfully incubated vectors into the scala media of the Cx26 knockout mice at P0-P1. Although auditory function did not show significant improvement in these mice, the cell death and the SGN degeneration were substantially reduced. Moreover, the TC could partially open in treated mice, which indicated that this gene therapy could overcome morphological abnormality in cCx26 KO mice. The exogenous gene expression takes about one week to reach the maximal stable level, thus they considered the unsatisfied hearing may be caused by missing the best critical time window for rescue [20].

In conclusion, our different postnatal Cx26 KD models showed diverse patterns of hearing loss and cell degeneration. The diversities among these models may further elucidate the mechanism of Cx26 involved in cochlear development. Considering new gene therapies, this study may provide a novel mouse model for early intervention on Cx26 mutants.

Acknowledgments

This work was supported by grants from the National Nature Science Foundation of China (81230021), the Major State Basic Research Development Program of China (973 Program) (2011CB504504) and the National Nature Science Foundation of China (30730094 and 81000408).

References

[1] D. Kelsell, J. Dunlop, H. Stevens, N. Lench, J. Liang, G. Parry, R. Mueller, I. Leigh, Connexin 26 mutations in hereditary non-syndromic sensorineural deafness, Nature 387 (1997) 80–83.
[2] M. RamShankar, S. Girirajan, O. Dagan, H.R. Shankar, R. Jalvi, R. Rangasayee, K. Avraham, A. Anand, Contribution of connexin26 (GJB2) mutations and founder effect to non-syndromic hearing loss in India, J. Med. Genet. 40 (2003) e68.
[3] R.J. Morell, H.J. Kim, L.J. Hood, L. Goforth, K. Friderici, R. Fisher, G. Van Camp, C.I. Berlin, C. Oddoux, H. Ostrer, Mutations in the connexin 26 gene (GJB2) among Ashkenazi Jews with nonsyndromic recessive deafness, N. Engl. J. Med. 339 (1998) 1500–1505.
[4] A.D. Martinez, R. Acuna, V. Figueroa, J. Maripillan, B. Nicholson, Gap-junction channels dysfunction in deafness and hearing loss, Antioxid. Redox Signal. 11 (2009) 309–322.
[5] M. Cohen-Salmon, T. Ott, V. Michel, J.P. Hardelin, I. Perfettini, M. Eybalin, T. Wu, D.C. Marcus, P. Wangemann, K. Willecke, C. Petit, Targeted ablation of connexin26 in the inner ear epithelial gap junction network causes hearing impairment and cell death, Curr. Biol. 12 (2002) 1106–1111.
[6] T. Kudo, S. Kure, K. Ikeda, A.-P. Xia, Y. Katori, M. Suzuki, K. Kojima, A. Ichinohe, Y. Suzuki, Y. Aoki, Transgenic expression of a dominant-negative connexin26 causes degeneration of the organ of Corti and non-syndromic deafness, Hum. Mol. Genet. 12 (2003) 995–1004.
[7] B.C. Cox, Z. Liu, M.M. Lagarde, J. Zuo, Conditional gene expression in the mouse inner ear using Cre-loxP, J. Assoc. Res. Otolaryngol. 13 (2012) 295–322.
[8] Y. Wang, Q. Chang, W. Tang, Y. Sun, B. Zhou, H. Li, X. Lin, Targeted connexin26 ablation arrests postnatal development of the organ of Corti, Biochem. Biophys. Res. Commun. 385 (2009) 33–37.
[9] Y. Sun, W. Tang, Q. Chang, Y. Wang, W. Kong, X. Lin, Connexin30 null and conditional connexin26 null mice display distinct pattern and time course of cellular degeneration in the cochlea, J. Comp. Neurol. 516 (2009) 569–579.
[10] Y. Qu, W. Tang, B. Zhou, S. Ahmad, Q. Chang, X. Li, X. Lin, Early developmental expression of connexin26 in the cochlea contributes to its dominate functional role in the cochlear gap junctions, Biochem. Biophys. Res. Commun. 417 (2012) 245–250.
[11] C.M. Frenz, T.R. Van De Water, Immunolocalization of connexin 26 in the developing mouse cochlea, Brain Res. Rev. 32 (2000) 172–180.
[12] R. Guillery, On counting and counting errors, J. Comp. Neurol. 447 (2002) 1–7.
[13] D. Forrest, T.A. Reh, A. Rüsch, Neurodevelopmental control by thyroid hormone receptors, Curr. Opin. Neurobiol. 12 (2002) 49–56.
[14] Q. Chang, W. Tang, S. Ahmad, B. Zhou, X. Lin, Gap junction mediated intercellular metabolite transfer in the cochlea is compromised in connexin30 null mice, PLoS One 3 (2008) e4088.
[15] F. Anselmi, V.H. Hernandez, G. Crispino, A. Seydel, S. Ortolano, S.D. Roper, N. Kessaris, W. Richardson, G. Rickheit, M.A. Filippov, H. Monyer, F. Mammano, ATP release through connexin hemichannels and gap junction transfer of second messengers propagate Ca2+ signals across the inner ear, Proc. Natl. Acad. Sci. USA 105 (2008) 18770–18775.
[16] D.A. Cotanche, C.L. Kaiser, Hair cell fate decisions in cochlear development and regeneration, Hear Res. 266 (2010) 18–25.
[17] C. Liang, Y. Zhu, L. Zong, G.-J. Lu, H.-B. Zhao, Cell degeneration is not a primary causer for Connexin26 (GJB2) deficiency associated hearing loss, Neurosci. Lett. 528 (1) (2012) 36–41.
[18] G. Crispino, G. Di Pasquale, P. Scimemi, L. Rodriguez, F. Galindo Ramirez, R.D. De Siati, R.M. Santarelli, E. Arslan, M. Bortolozzi, J.A. Chiorini, F. Mammano, BAAV mediated GJB2 gene transfer restores gap junction coupling in cochlear organotypic cultures from deaf Cx26Sox10Cre mice, PLoS One 6 (2011) e23279.
[19] Y. Wang, Y. Sun, Q. Chang, S. Ahmad, B. Zhou, Y. Kim, H. Li, X. Lin, Early postnatal virus inoculation into the scala media achieved extensive expression of exogenous green fluorescent protein in the inner ear and preserved auditory brainstem response thresholds, J. Gene Med. 15 (2013) 123–133.
[20] Q. Yu, Y. Wang, Q. Chang, J. Wang, S. Gong, H. Li, X. Lin, Virally expressed connexin26 restores gap junction function in the cochlea of conditional Gjb2 knockout mice, Gene Ther. 21 (2014) 71–80.